

Stator Current Spectral content of an Induction Motor taking into account Saturation Effect

Abstract. The work presented in this paper focuses on the spectral content of the stator current in the presence of the saturation effect. To do this, it is necessary to have a mathematical model of the reliable induction machine capable of predicting its behavior in the presence of saturation. The approach of the modified winding function is among the most significant methods because it takes into account the actual distribution of the windings in the stator slots. For this purpose, a series of simulations are carried out to highlight the spectral content of the stator current of the induction squirrel cage motor in the various cases of operation with and without taking into account the saturation effect.

Streszczenie. Analizowano charakterystyki widmowe prądu stojana silnika indukcyjnego w stanie nasycenia. Opracowano też model matematyczny silnika umożliwiający przeprowadzenie symulacji. Porównano wyniki symulacji z uwzględnieniem nasycenia i bez. **Analiza widmowa prądu stojana silnika indukcyjnego z uwzględnieniem efektu nasycenia**

Keywords: Induction motor, Modified winding function, Saturation, Spectrum, stator current.

Słowa kluczowe: silnik indukcyjny, analiza widmowa, nasycenie rdzenia.

Introduction

The asynchronous machine occupies a very important area in industry and transport. It is appreciated for its robustness, its low cost of purchase and its low maintenance. The machine requires only one power source [1].

In an electric machine, the magnetic circuit acts as a flux channel to direct the magnetic field in the gap. In this magnetic circuit, energies of different kinds are transformed, stored, exchanged and dissipated. The performance of the modeling and simulation of the machine's operation is directly related to the precision with which all these forms of energy are simultaneously evaluated [2]. This is the reason why the model proposed in this study takes into account the phenomenon of saturation. The approach of the modified winding functions is used in the present work. The spectral content in the case without saturation and with saturation is studied in this paper.

Modeling the healthy machine

In this work, a three-phase cage induction motor is considered. The rotor consists of N_b insulated bars, uniformly distributed on the surface of the rotor and short-circuited by two rings [3].

We used a model where the cage is considered as a mesh circuit Fig.1. The number of differential equations obtained is equal to the number of bars plus one (in order to take into consideration one of the two rings) [4, 5, 6].

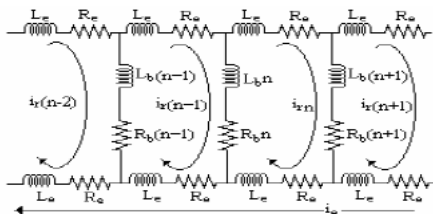


Fig.1. Mesh circuit of the cage rotor

Under the classical assumptions of simplifications, the mathematical model of the machine is given by the equations of the voltages below:

$$(1) \quad [V_s] = [R_s][I_s] + \frac{d[\Psi_s]}{dt}$$

$$(2) \quad [V_r] = [R_r][I_r] + \frac{d[\Psi_r]}{dt}$$

where $[\Psi_s]$ and $[\Psi_r]$ represent the vectors grouping the total flux through the stator and rotor windings respectively. $[I_s]$ and $[I_r]$ are the corresponding currents, with:

$$(3) \quad [I_s] = [i_{sa} \ i_{sb} \ i_{sc}]^T$$

$$(4) \quad [I_r] = [i_{r1} \ i_{r2} \ i_{r3} \ \dots \ i_{rmb} \ i_{re}]^T$$

$$(5) \quad [\Psi_s] = [L_{ss}][I_s] + [L_{sr}][I_r]$$

$$(6) \quad [\Psi_r] = [L_{rr}][I_r] + [L_{rs}][I_s]$$

By grouping equations (1) and (2) in the same matrix equation, we obtain:

$$(7) \quad [V] = [R][I] + [L] \frac{d[I]}{dt} + \omega_r \frac{d[L]}{dt} [I]$$

Such that:

$$(8) \quad [V] = \begin{bmatrix} [V_s] \\ [V_r] \end{bmatrix} \quad [R] = \begin{bmatrix} [R_s] & [0] \\ [0] & [R_r] \end{bmatrix} \quad [L] = \begin{bmatrix} [L_{ss}] & [L_{sr}] \\ [L_{rs}] & [L_{rr}] \end{bmatrix} \quad [I] = \begin{bmatrix} [I_s] \\ [I_r] \end{bmatrix}$$

The mechanical equations of the movement is added to the system of electrical equations and this is the purpose of doing an electromechanical study of the machine's operation.

$$(9) \quad J_T \frac{d\omega_r}{dt} = T_e - T_c$$

and

$$(10) \quad \omega_r = \frac{d\theta_r}{dt}$$

or

- J_T : Moment of total inertia on the motor shaft
- T_c : Load torque
- T_e : Electromagnetic torque produced by the machine

For a linear magnetic circuit, the Co-energy is equal to the energy stored. Hence, the torque equation is given as:

$$(11) \quad T_e = \left[\frac{\partial W_{co}}{\partial \theta_r} \right]_{(I_s, I_r \text{ constants})}$$

with:

$$(12) \quad W_{co} = \frac{1}{2} \begin{bmatrix} I_s^t & I_r^t \end{bmatrix} \begin{bmatrix} L_{ss} & L_{sr} \\ L_{rs} & L_{rr} \end{bmatrix} \begin{bmatrix} I_s \\ I_r \end{bmatrix}$$

This finally gives the expression of the electromagnetic torque.

$$(13) \quad T_e = \frac{1}{2} I_s^t \frac{\partial L_{sr}}{\partial \theta_r} I_r + \frac{1}{2} I_r^t \frac{\partial L_{rs}}{\partial \theta_r} I_s$$

The combination of the electric equations (7) and the equations of motion (9), (10) and (13) leads to the global equation system [7]:

$$(14) \quad \begin{bmatrix} [v] \\ 0 \\ [T_e - T_c] \end{bmatrix} = \begin{bmatrix} [R] + \omega_r \frac{\partial}{\partial \theta_r} [L] & [0] \\ [0] & [1] \\ [0] & k_f \end{bmatrix} \begin{bmatrix} [i] \\ [\theta_r] \\ [0] \end{bmatrix} + \begin{bmatrix} [L] & [0] \\ [0] & J_T \end{bmatrix} \frac{d}{dt} \begin{bmatrix} [i] \\ [\theta_r] \end{bmatrix}$$

This gives:

$$(15) \quad \frac{d}{dt} \begin{bmatrix} [i] \\ [\theta_r] \\ [0] \end{bmatrix} = \begin{bmatrix} [L] & [0] \\ [0] & J_T \end{bmatrix}^{-1} \begin{bmatrix} [v] \\ 0 \\ [T_e - T_c] \end{bmatrix} - \begin{bmatrix} [R] + \omega_r \frac{\partial}{\partial \theta_r} [L] & [0] \\ [0] & [1] \\ [0] & k_f \end{bmatrix} \begin{bmatrix} [i] \\ [\theta_r] \\ [0] \end{bmatrix}$$

The system of equations obtained is $(n_b + 6)$ differential equations with variable coefficients, the inductances depend on the position of the rotor relative to the stator. To solve this system, it is necessary to have the values of the different inductances of the machine.

A. Calculation of inductances without saturation

All system inductances thus obtained are calculated using the modified winding function. [8]:

$$(16) \quad N(\varphi, \theta_r) = n(\varphi, \theta_r) - \frac{1}{2\pi(g^{-1}(\varphi, \theta_r))} \int_0^{2\pi} n(\varphi, \theta_r) g^{-1}(\varphi, \theta_r) d\varphi$$

From equation (16), and by performing the variable change $x = r\varphi$ and $x_r = r\theta_r$, everything comes back as if we referred to an orthonormal coordinate system of X and Z axes, where it is possible to imagine a plane representation of the machine. It is clear that x , in this case, translates well the linear displacement along the arc corresponding to the angular opening φ . Similarly with regard to x_r [9]. Knowing that N is the FMM per unit of current, the flux seen by the turns of a coil B_j due to the current passing through another coil A_i has for expression:

$$(17) \quad \phi_{B_j A_i} = \mu_0 \int_0^{2\pi r} \int_0^l N_{A_i}(x, z, x_r) n_{B_j}(x, z, x_r) g^{-1}(x, z, x_r) A_i dz dx$$

The inductance between any two coils will be:

$$(18) \quad L_{B_j A_i}(x_r) = \mu_0 \int_0^{2\pi r} \int_0^l N_{A_i}(x, z, x_r) n_{B_j}(x, z, x_r) g^{-1}(x, z, x_r) dz dx$$

From Figure. 2, the distribution functions of a stator coil and a rotor mesh can be defined as follows:

$$(19) \quad n_{A_i}(x, z, x_r) = \begin{cases} N_s & x_{i1} < x < x_{i2}, 0 < z(x) < l \\ 0 & \text{at the remaining interval} \end{cases}$$

$$(20) \quad n_{r_j}(x, z, x_r) = \begin{cases} 1 & x_{1j} < x < x_{2j}, 0 < z(x) < l \\ 0 & \text{at the remaining interval} \end{cases}$$

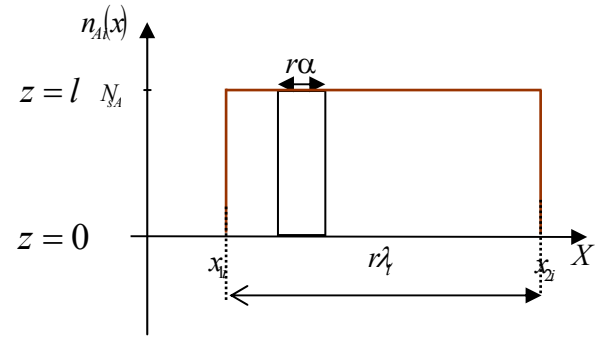


Fig.2. Distribution function of a stator coil. A_i .

The analytic integration gives us the results recorded in table 1. For each given interval we have a value of the mutual inductance which depends on x_r .

Table 1. Calculated values of mutual inductance between the 1st stator coil and the 1st rotor mesh

Distance x_r in (mm)	Inductance $L_{a_i r}$ (H)
$0 \leq x_r < x_{i1} - r\alpha_r$	$-\frac{\mu_0 r l}{2\pi g_0} N_s \alpha_r \lambda$
$x_{i1} - r\alpha_r \leq x_r < x_{i1}$	$\frac{\mu_0 r l}{g_0} N_s (x_r - x_{i1} + \alpha_r (1 - \lambda / 2\pi))$
$x_{i1} \leq x_r < x_{i2} - r\alpha_r$	$\frac{\mu_0 r l}{g_0} N_s \alpha_r (1 - \lambda / 2\pi)$
$x_{i2} - r\alpha_r \leq x_r < x_{i2}$	$\frac{\mu_0 r l}{g_0} N_s (-x_r + x_{i2} - (\lambda \alpha_r / 2\pi))$
$x_{i2} \leq x_r < 2\pi r$	$-\frac{\mu_0 r l}{2\pi g_0} N_s \alpha_r \lambda$

B. Calculation of inductances with saturation

The calculation of the inductances is done in the same way as in the case of a uniform air gap except for the inverse of the air gap function which is replaced by the following equation [10, 11, 12, 13]:

$$(21) \quad g^{-1}(\varphi, \theta_r, z) = \frac{1}{g} [1 + k_{gsat} \cos(2(p\varphi - \theta_f))]]$$

$$\text{With:} \quad k_{gsat} = \frac{2(k_s - 1)}{3k_s} \quad g' = g_0 \frac{3k_s}{k_s + 2}$$

where, φ is the position of the stator, θ_f is the position of the gap flux, k_s is the saturation factor which is determined by the ratio between the fundamental components of the gap voltage in the unsaturated case and the saturated case, g' is the modified average value of the gap in the presence of saturation. The analytic integration gives us the results recorded in table 2. For each given interval one has a value of the mutual inductance which depends on x_r and x_f .

Table 2. Calculated values of mutual inductance between the first stator coil and the first rotor mesh with saturation

Distance x_r in (mm)	Inductance $L_{a,r}$ (H)
$0 \leq x_r < x_{i1} - r\alpha_r$	$-\frac{\mu_0 r l}{2\pi g_0} N_s \lambda \left[\alpha_r + \frac{k_{sat}}{2p} \sin(2(p(x_r + \alpha_r) - x_f)) - \sin(2(px_r - x_f)) \right]$
$x_{i1} - r\alpha_r \leq x_r < x_{i1}$	$\frac{\mu_0 r l}{g_0} N_s \left[(x_r - x_{i1} + \alpha_r(1 - \lambda/2\pi)) + \frac{k_{sat}}{2p} \left[\frac{\lambda}{2p} \sin(2(px_r - x_f)) + \left(1 - \frac{\lambda}{2p}\right) \sin(2(p(x_r + \alpha_r) - x_f)) - \sin(2(px_{i1} - x_f)) \right] \right]$
$x_{i1} \leq x_r < x_{i2} - r\alpha_r$	$\frac{\mu_0 r l}{g_0} N_s (1 - \lambda/2\pi) \left[\alpha_r + \frac{k_{sat}}{2p} \sin(2(p(x_r + \alpha_r) - x_f)) - \sin(2(px_r - x_f)) \right]$
$x_{i2} - r\alpha_r \leq x_r < x_{i2}$	$\frac{\mu_0 r l}{g_0} N_s \left[(-x_r + x_{i2} - (\lambda\alpha_r/2\pi)) + \frac{k_{sat}}{2p} \left[-\frac{\lambda}{2p} \sin(2(p(x_r + \alpha_r) - x_f)) + \left(\frac{\lambda}{2p} - 1\right) \sin(2(px_r - x_f)) + \sin(2(px_{i2} - x_f)) \right] \right]$
$x_{i2} \leq x_r < 2\pi r$	$-\frac{\mu_0 r l}{2\pi g_0} N_s \lambda \left[\alpha_r + \frac{k_{sat}}{2p} \sin(2(p(x_r + \alpha_r) - x_f)) - \sin(2(px_r - x_f)) \right]$

Fig. 3 shows the magnetization inductance of stator phase as a function of the position of the without (a) and with saturation (b).

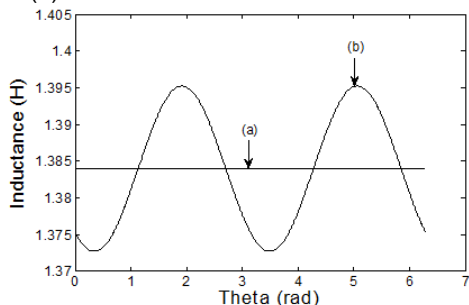


Fig.3. Magnetization inductance as a function of the position of the stator. (a) without saturation, (b) with saturation

The mutual inductance between the stator phases with and without the saturation effect is also calculated and shown in Figure 4. (a-b).

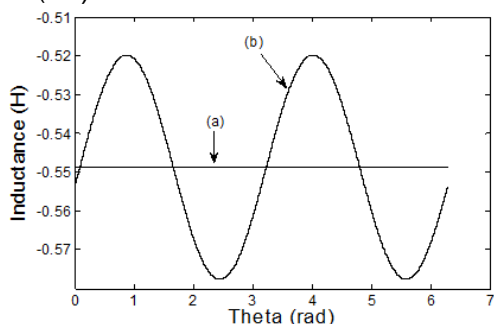


Fig.4. Mutual inductance between the stator phases 'a' and 'b' (a) without saturation, (b) with saturation.

It can be noted that the inductance of the stator becomes constant when the saturation factor is zero (without saturation), the saturation effect becomes greater when the inductance becomes sinusoidal and variable as a function of the position of the gap.

Figures 5. (a-b) and 6. respectively show respectively the magnetization inductances of the first rotor mesh, the mutual inductance between the first mesh and the third

mesh, the mutual stator-rotor mutual inductance without the saturation effect.

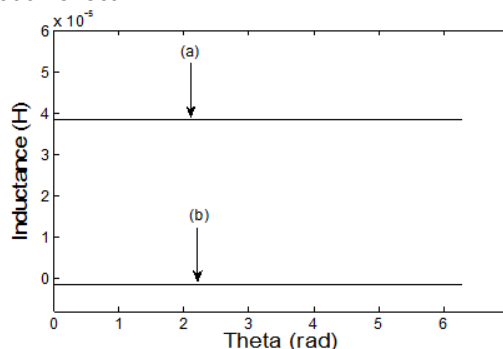


Fig.5. Magnetizing and mutual rotor inductance without saturation 'a' and 'b' (a) magnetizing, (b) mutual

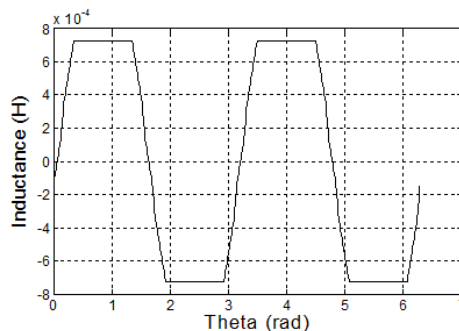


Fig.6. Mutual inductance between the first stator phases 'a' and the first rotor cell without saturation.

Figures. 7, 8, 9 respectively show the stator-rotor mutual inductance, the magnetization inductance of the first rotor mesh and the mutual inductance between the first mesh and the third mesh with the saturation effect as a function of the position of the rotor and that of the gap.

Taking into account the saturation in the calculation of the inductances, allowed us to see the considerable variations of the latter in their amplitudes and their shapes compared to the conventional model (without saturation).

It can be concluded that the modeling of our induction machine, taking into account the effect of saturation, enabled us to calculate the inductances in a way closer to

the real case of the distribution of the magnetic flux in the gap. To better see the behavior of the induction machine, a detailed study, taking into account the saturation, will be presented through the simulation results.

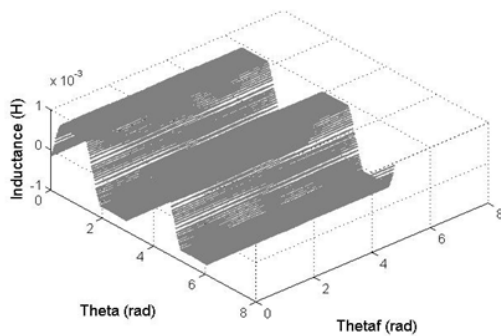


Fig.7. Mutual inductance between the first stator phases 'a' and the first rotor mesh with saturation

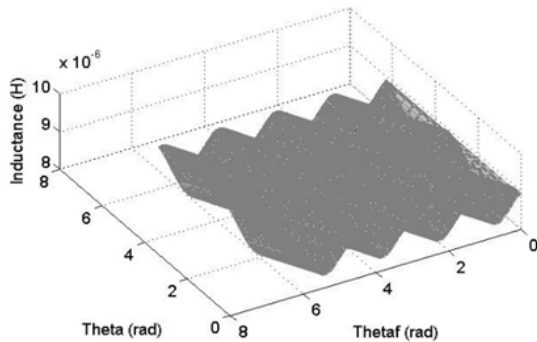


Fig.8. Magnetizing inductance of the first rotor mesh with saturation

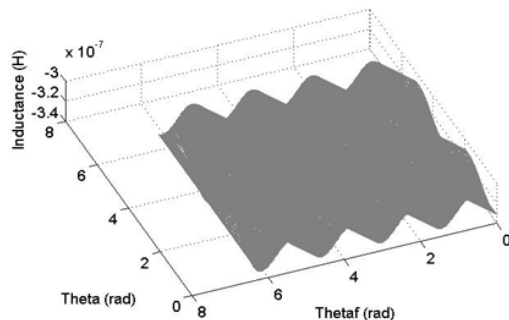


Fig.9. Mutual inductance between the first rotor mesh and the second rotor mesh with saturation.

Simulation results

Once the model of our squirrel cage induction motor is structured for different cases, we can now approach the simulation of it. A program written in the Matlab environment has been developed in our laboratory. The latter makes it possible to highlight the behavior of the induction motor without and with the saturation effect. It should be noted that the simulation presented in this paper is performed with a nominal load torque of 20Nm. The parameters of the induction squirrel cage motor used are given in the appendix.

A. Simulation of the healthy motor without taking into account saturation

Figure.10 gives the spectrum of the stator current of the phase A. It can be noticed that this spectrum is composed of three important harmonics from amplitude point of view, there is of course the fundamental harmonic (50hz) and two other harmonics of frequencies (586.6Hz and 686.5Hz). These harmonics represent the rotor notch harmonics.) These harmonics represent those of the rotor slot and occur

in pairs at regular intervals and whose expression is given by the following equation:

$$(22) \quad f_{he} = \left[\frac{kN_b}{p} (1-g) \pm v \right] f_s$$

With f_s the supply frequency, p the number of pairs of poles, $k = 1, 3, \dots, N_b$ the number of rotor bars, $v = \pm 1, \pm 3, \dots$ and g the slip.

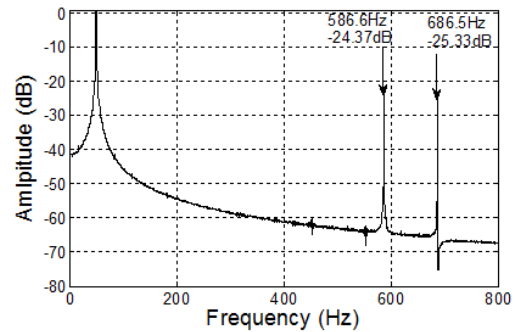


Fig.10. Spectrum of the stator current for the case of a healthy motor operation without taking into account the saturation effect.

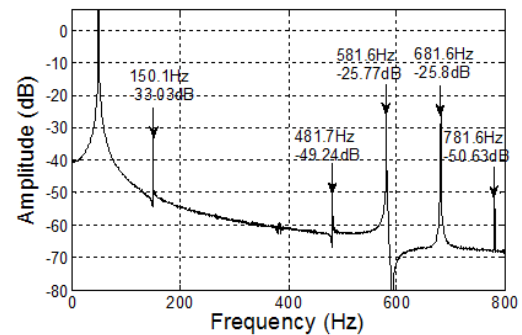


Fig.11. Spectrum of the stator current for the case of an operation without and with the saturation effect.

B. Simulation of the healthy motor with saturation

Figure.11 shows the spectrum of the current for the case of taking into account the effect of saturation; it can be noted that there is the appearance of a harmonic at the frequency 150Hz. The latter will create higher order harmonics at frequencies (481.7Hz and 781.6Hz), which can be verified using equation (22) substituting v by ± 3 . The presence of these harmonics shows that the harmonic created by the saturation in turn creates its own harmonics of rotor slots.

Conclusion

In this work, the spectral content of the stator current in the presence of the saturation effect based on the concept of modified winding function is presented. This model used two approaches first, the winding function to account for the effect of space harmonics and the second to account for the saturation effect. The simulation results show that the saturation is manifested by the creation of the 3rd harmonic as well as the harmonics of rotor slots relative to this harmonic.

It should be noted that the saturation is manifested by the creation of harmonics in the spectrum of the stator current at the same frequencies as those created by the imbalance of the power supply and the short-circuit fault between stator turns.

Appendix

Motor parameters used	
Rated power	3 kw
Power frequency	50 Hz
rotational speed	1440tr/mn
Stator phase resistance	5.5 Ω
Stator leakage inductance	0.063 H.
Rotor bar resistance	150 $\mu\Omega$
Short circuit ring resistance	1.59 $\mu\Omega$
Rotor bar leakage inductance	0.603 nH
Short circuit ring leakage inductance	2 nH
Moment of inertia	0.058 kgm ²
Coefficient of friction length	5 10 ⁻⁴ Nm
Thickness of gap	130mm
Medium radius	0.18mm
Number of turns	44mm
Number of stator slots	54 spires.
Number of bars	36 encoches.
	28 barres.

Authors: Phd student Miloud Harir, Laboratory Diagnostic Group, LDEE, University of Sciences and Technology of Oran, -Mohamed Boudiaf - Faculty of Electrical Engineering BP 1505 Al Mnaouar, 31000 Oran, Algeria. Email: miloud_ing@yahoo.fr; miloud.harir@univ-usto.dz
 Prof. Azeddine Bendiabdellah, Laboratory Diagnostic Group, LDEE, University of Sciences and Technology of Oran, -Mohamed Boudiaf - Faculty of Electrical Engineering BP 1505 Al Mnaouar, 31000 Oran, Algeria. Email: bendiaz@yahoofr

REFERENCES

- [1]. Hubert Razik et Gaëtan Didier, "Notes de cours sur le diagnostic de la machine asynchrone", Notes de cours, I.U.F.M. de Lorraine, Maxeville, 7 janvier 2003.
- [2] J.P.Lecoq, B.Cassoret and J.F.Brudny,"Distinction of Tothing and Saturation Effects on Magnetic Noise of Induction Motors", Progress in Electromagnetics Research, Vol.112, pp.125-137, 2011.
- [3] Noureddine Benouzza, Ahmed Hamida Boudinar, Azeddine Bendiabdellah, Mohammed El-amine Khodja, "Slot harmonic frequency detection as a technique to improve stator current spectrum approach for broken rotor bars fault diagnosis " ,ACEMP-OPTIM-Electromotion 2015 Conference, Side - Turkey 2-4 September 2015
- [4] D.Bispo, L.M.Neto, J.T.Resende and D.A.Andrade, "A New Strategy for Induction Machines Modeling Taking into account the Magnetic Saturation", IEEE Trans. Ind. Appl., vol.37, No.6, pp. 1710-1719, Nov/Dec. 2001.
- [5] H. Razik et G.Dédier , " Notes de Cours sur le Diagnostic de la Machine Asynchrone ", Université Henri Poincaré, Nancy. H.Austin and George.
- [6] N.Benouzza, A.Benyettou and A.Bendiabdellah., "An Advanced PARK's Vectors Approach for Rotor Cage Diagnosis, Proceeding of CNGE 2004 01, Université Ibn Khaldoun de Tiaret.
- [7] V.Donesco, A.Charette, Z.Yao and V.Rajagoplan, " Modeling and Simulation of Asaturated Induction Motors in Phase Quantities", IEEE Trans. Energy Conversion, vol.14, No.3, pp. 386-393, Sept.1999.
- [8] J. Faiz and I. Tabatabaei, "Extension of winding function theory for nonuniform air-gap in electric machinery", IEEE Trans. Magnetics, vol. 38, no. 6, November 2002, pp. 3654-3657
- [9] A.Ghoggal, S.E. Zouzou, H.Razik, M.Sahraoui and D.A.H. Hamida, "Application of the Convolution Theorem for the Modeling of Saturated Induction Motors", 36th Annual Conf. on IEEE Ind. Electronics Society, 7-10 Nov. 2010.
- [10] A.Chaouch, A.Bendiabdellah, P.Remus, R.Raphael and P.L.Jean "Mixed Eccentricity Fault Diagnosis in Saturated Squirrel Cage Induction Motor using Instantaneous Power Spectrum Analysis" Przegląd Elektrotechniczny, R. 92 NR 7/2016.
- [11] G.Joksimović, "Line current spectrum analysis in saturated three-phase cage induction machine," Electrical Engineering, Springer Verlag, Vol.91, No.8, pp.425-437, April 2010.
- [12] S.Nandi. "An Extended Model of Induction Machines with Saturation suitable for Fault Analysis". IEEE Trans. Energy Conversion, vol.16, pp. 253-260, Sept.2003.
- [13] S.Nandi. "Detection of Stator Faults in Induction Machines Using Residual Saturation Harmonics". IEEE Trans. Ind. Appl., vol. 42, no. 5, September/October 2006.